Summary Report of HERO WEC Test Article for Waves to Water: Electrical Power Take-Off

Aryana Nakhai, Ben McGilton, and Scott Jenne

National Renewable Energy Laboratory

NREL is a national laboratory of the U.S. Department of Energy
Office of Energy Efficiency & Renewable Energy
Operated by the Alliance for Sustainable Energy, LLC

This report is available at no cost from the National Renewable Energy Laboratory (NREL) at www.nrel.gov/publications.

Contract No. DE-AC36-08GO28308

Technical Report
NREL/TP-5700-83621
September 2022

Summary Report of HERO WEC Test Article for Waves to Water: Electrical Power Take-Off

Aryana Nakhai, Ben McGilton, and Scott Jenne

National Renewable Energy Laboratory

Suggested Citation
Nakhai, Aryana, Ben McGilton, and Scott Jenne. 2022. *Summary Report of HERO WEC Test Article for Waves to Water: Electrical Power Take-Off.* Golden, CO: National Renewable Energy Laboratory. NREL/TP-5700-83621.
https://www.nrel.gov/docs/fy22osti/83621.pdf.

NREL is a national laboratory of the U.S. Department of Energy
Office of Energy Efficiency & Renewable Energy
Operated by the Alliance for Sustainable Energy, LLC

This report is available at no cost from the National Renewable Energy Laboratory (NREL) at www.nrel.gov/publications.

Contract No. DE-AC36-08GO28308

Technical Report
NREL/TP-5700-83621
September 2022

National Renewable Energy Laboratory
15013 Denver West Parkway
Golden, CO 80401
303-275-3000 • www.nrel.gov

NOTICE

This work was authored by the National Renewable Energy Laboratory, operated by Alliance for Sustainable Energy, LLC, for the U.S. Department of Energy (DOE) under Contract No. DE-AC36-08GO28308. Funding provided by U.S. Department of Energy Office of Energy Efficiency and Renewable Energy Water Power Technologies Office. The views expressed herein do not necessarily represent the views of the DOE or the U.S. Government.

Cover Photos by Dennis Schroeder: (clockwise, left to right) NREL 51934, NREL 45897, NREL 42160, NREL 45891, NREL 48097, NREL 46526.

List of Acronyms

Ah	ampere-hour
CBS	cost breakdown structure
DAQ	data acquisition
DOE	U.S. Department of Energy
HERO	hydraulic and electric reverse osmosis
kW	kilowatt
kWh	kilowatt-hour
MPPT	maximum point power tracking
mV	millivolt
N·m	newton-meter
NREL	National Renewable Energy Laboratory
PTO	power take-off
rpm	revolutions per minute
V	volt
W	watt
WBjr	Whizbang Junior
WEC	wave energy converter
WPTO	Water Power Technologies Office

Executive Summary

The U.S. Department of Energy's Water Power Technologies Office launched the Waves to Water Prize, initiated in 2019 and concluded in 2022, to encourage the development of small, modular, cost-competitive wave-powered desalination systems and to accelerate research endeavors for wave energy converters (WECs) capable of providing clean water in disaster relief scenarios. To better understand some of the challenges in developing a WEC, while following many of the constraints the competitors in the prize challenge were held to, the prize offered an opportunity for the National Renewable Energy Laboratory to design and develop a test article, referred to as the hydraulic and electric reverse osmosis (HERO) WEC. There were many lessons learned throughout the design, fabrication, and testing of the HERO WEC device. These takeaways have led to a better understanding of the research needs in wave energy, which are difficult to learn in a modeling and simulation environment. The intent of this report is to provide the public with a summary of the electrical subsystem designed for the HERO WEC as well as highlight the technical limitations of fabricating a WEC with a reliable electrical power take-off at this scale.

Table of Contents

List of Figures

List of Tables

1 Background

Supported by the U.S. Department of Energy (DOE) and administered by the National Renewable Energy Laboratory (NREL), the Waves to Water Prize encouraged four competitors to develop a small, modular, cost-competitive wave-powered desalination system capable of providing clean water in disaster relief scenarios. In efforts to reduce the deployment risk for the competitors and collect data to inform prize activities, NREL designed, fabricated, and deployed the hydraulic and electric reverse osmosis wave energy converter (HERO WEC) test article in February 2022 at Jennette's Pier in North Carolina's Outer Banks, where the prize competition was later hosted in April 2022. Although NREL was not competing in the prize, the HERO WEC test article was designed to follow the same parameters and limitations the competitors were required to adhere to. Since the competitors' devices consisted of both hydraulic and electric power take-off (PTO) configurations, NREL designed the test article to be a modular system that can utilize either an electrical or hydraulic PTO system to power a desalination device. The test article can convert mechanical work to either hydraulic or electrical energy by harnessing energy from waves via a rotary output shaft. This report describes the electrical subsystem, in which a rotary generator powers a submersible pump via an electrical cable. The HERO WEC is a nonproprietary design—every aspect of the design is made publicly available for other developers to learn from and understand, including the physical designs, nonproprietary cost data, and electrical drawings developed for the build of the device.

2 Overview of Electrical System

2.1 Description

The system layout for the final design for the electrical system is shown as a block diagram in Figure 1. As shown, the main power electronic components used in the design of the electrical PTO are an AC rotary generator, a rectifier, a charge controller, batteries, and an inverter used to power the load, which is an AC submersible pump. Through hydrodynamic action, the WEC harnesses the energy predominantly from the heave motion of the waves and converts it into rotational movement to drive an AC electrical generator by means of a winch-pulley system. The generator's AC output is then transported back to shore via an electrical cable and is converted to DC power through a bridge rectifier to power a maximum point power tracking (MPPT) charge controller and lead-acid batteries, which are used to maintain a 24-volt (V) DC bus for continuous inverter operation. The inverter is used to convert the 24-V DC power to 120-V AC to power an AC submersible pump, which provides the necessary flow and pressure to the reverse osmosis desalination system.

The charge controller's function is to regulate the voltage and current from the generator to prevent overcharging and excessive discharging of the battery. For this design, an MPPT type charge controller was used, which is an algorithm included in some controllers to extract the maximum available power from a variable power source by operating at the most efficient voltage, or the maximum power point. It follows the output of the generator, compares it to battery voltage, and adjusts the input voltage to maintain the most efficient power for the system (Phocos 2015).

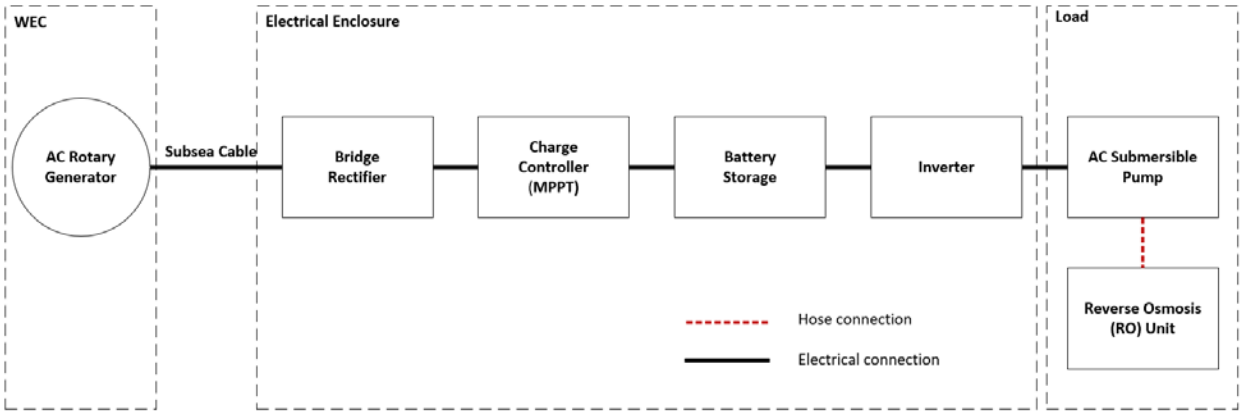

Figure 1. Block diagram of electrical system layout

2.2 Electrical Design Details

In efforts to follow the prize rules, which limited battery storage to 0.5 kilowatt-hour (kWh), this design started with two 12-V, 21-ampere-hour (Ah) absorbent glass mat deep-cycle batteries (PDC-12200) in series to create a 24-V DC bus. The charge controller needed to operate with the 24-V DC bus and, due to the uncertainty with wave conditions and amplitudes, needed to have a wide input voltage range to handle substantial voltage fluctuation from the generator. The charge controller selected was MidNite Solar's MPPT charge controller (CLASSIC250), with an operating voltage range between 32 and 250 V and power output of 1.8 kW for a 24-V DC

system. The inverter was sized for both the battery voltage and the pump's input voltage. The peak voltage of the generator was designed such that the voltage would not exceed the 250 V in the most extreme sea state scenarios. Due to the limited availability of generators that can function in a marine environment while meeting the voltage and speed requirements, the generator was the only component that was custom designed. It is a 3-kW rated machine with 9 pole pairs and was designed for 120 V per 1,000 revolutions per minute (rpm), 30 newton-meters (N·m) nominal torque, and 50 N·m peak torque. The peak torque was specifically selected such that, in the event of a sudden maximum current draw due to controller error or fault, the force applied by the PTO would not lift the WEC's anchor, and the device would not be compromised. Table 1 includes the details the performance specifications of the generator, with the frequency of the AC current production in the last column. It is important to note that, while the machine's nameplate rating is 3 kW, the charge controller sets a whole system maximum rating of 1.8 kW. The generator was also designed to be completely marinized with seals, coatings, and protection against water because it is the one electrical component that sits on the WEC in the water, as illustrated in Figure 1. Details on the assembly configuration and dimensions of the custom generator can be found in Appendix A.

Table 1. Custom Generator Performance and Design Specifications

Speed (rpm)	No Load DC Voltage (V)	DC Voltage (V)	DC Current (amperes [A])	Power (watts [W])	Efficiency (%)	Torque (N·m)	Frequency (hertz [Hz])
400	55	48	25	1,200	87	32.9	60
500	68	60	25	1,500	88	32.5	75
600	82	72	25	1,800	89	32.2	90
700	96	84	25	2,100	90	31.9	105
800	109	96	25	2,400	91	31.6	120
900	123	108	25	2,700	92	31.3	135
1,000	137	120	25	3,000	92	31.0	150
1,100	150	132	25	3,300	92	31.3	165

2.3 Component Sizing and Limitations

Developing and testing the HERO WEC enabled a better understanding of the research needs in wave energy. There were many lessons learned throughout the design, fabrication, and testing process. These takeaways have led to a better understanding of the research needs in wave energy, which are difficult to learn in a modeling and simulation environment and are not typically made publicly available for other developers to benefit from. As with any electrical design, the sizing of components is driven by various limitations.

A key limitation in the design of the electrical system was the relatively low battery capacity of 0.5 kWh, which was set by the prize rules. The 0.5 kWh capacity was set by the prize rules to ensure that all systems used wave energy and did not develop a battery-powered desalination unit. The design of the electrical system started with a 0.5-kWh battery bank (Power Sonic, PDC-12200), but during testing the batteries were found to be too small for the current draw

from the inverter, pump, and charge controller, and were not sufficient to maintain power for both the load and control components. Because the pump was an induction-type motor, the initial starting current was about 5 times higher than its steady-state condition. This greatly exceeded the charge controller's maximum current, requiring the batteries to supply the majority of the current, causing the voltage to drop below the minimum operating points for both the inverter and charge controller. Therefore, the original batteries were replaced with batteries of 2-kWh capacity (Optima, DH7) to keep the system on and functioning.

Other limitations in the design of the electrical subsystem were due to electrical specifications and limits associated with commercial off-the-shelf components. For example, charge controllers are typically designed for more steady-state applications, like solar and wind energy technology, and have a tight operating voltage range. For the charge controller selected and used in the HERO WEC design, the operating voltage range was between 32 V and 250 V. This forced a narrow operating range where the controller did not turn on until energetic sea states, reducing both the total potential energy harvested and the maximum power generation of the system. This limitation highlighted the substantial need for bespoke power electronics and power conversion systems that can manage the wide range of operating conditions common to wave energy. Specifically, robust power electronics must be developed that are capable of sustained operation at very low power points, have high efficiency over a wide operating range, and are capable of continued operation through extreme, or peak, events.

2.4 Charge Controller Programming

Programming the charge controller properly is an important step in ensuring it delivers the appropriate charge profile to a battery bank. This section walks through the programming parameters for the MidNite Solar Classic 250 charge controller to charge the lead-acid batteries.

2.4.1 Battery Charge Stages

This charge controller operates on a four-stage charging cycle (bulk, absorption, float, and equalization), where each charge cycle describes the voltage and current relationship in a battery as the charger returns the energy capacity to the battery. These four stages are visually represented in Figure 2. Different battery chemistries, such as lead-acid, lithium-ion, etc., require different methods of charging. The first step in programming the charge controller was adjusting the absorb, equalize, and float voltages, which are taken from the battery manufacturer's data sheet.

The first stage is bulk charging, which is when the charge controller identifies if the battery is starting in a discharged state or not. If so, the controller operates in constant current mode where the charger's output current is maintained at a constant value and the battery voltage increases as it is being recharged. Approximately 80% of battery capacity is returned in this stage, which is commonly referred to as the constant-current region or the bulk stage.

The second stage is the absorb stage, which means that when the battery voltage reaches approximately 2.4 V per cell, or 14.7 V for the 12-V battery, the charge controller will maintain the absorb set point voltage until the batteries are charged and the battery current is allowed to reduce. Because there are two batteries in series, the absorb voltage was doubled (29.4 V) and programmed into the charge controller.

Following the absorb stage is the float stage, which specifies the voltage set point the battery is held at and maintained at approximately 2.3 V per cell, or 13.6 V for the 12-V battery. This voltage will maintain the full charge condition in the battery without overcharging the battery. Similar to the absorb voltage, the float voltage was doubled (27.2 V) and programmed into the charge controller.

The fourth and last stage is the equalize cycle, which is intended to bring all battery cells to an equal voltage by a deliberate overcharge of the controller. The goal is to return each battery cell to its optimal condition through a series of voltage-controlled chemical reactions inside the batteries. The equalization voltage was also doubled (30 V) and programmed into the charge controller.

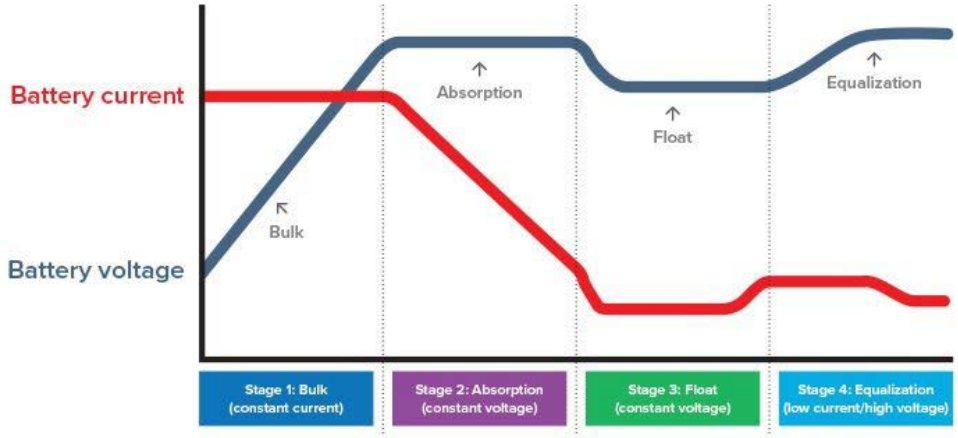

Figure 2. Four-stage battery charging cycle

2.4.2 Custom Power Curve

The next step in the setup was developing a custom power curve to be entered into the charge controller, which involves knowing the operational voltages of the charge controller. As described by the charge controller manufacturer, the minimum operating voltage is 133% of the battery voltage, which is about 32 V for a 24-V battery, and the maximum operating voltage is 250 V. With these set points in mind, the control strategy, or I-V curve, was developed from the 16 points displayed in Table 2. The P-V curve shown in Figure 3 is the electrical power ($P = V \times I$) relative to the increasing voltage. In this application, the speed of the generator, and therefore the induced voltage, is related to the wave height and wave period.

A limitation of the programming options is that the charge controller does not allow the user to enter a step value below or equal to the previous step value. Because most waves were expected to be in the lower range of wave heights, the I-V curve was designed to have a sharp increase to the maximum rated power (~1.8 kW) to maximize power output, which is reached after step 5, as shown in Table 2. Once the power curve exceeds 1.8 kW, this represents the theoretical maximum power that the charge controller would draw if it could, but because the system physically cannot draw the amount of current after step 5, it acts as a constant draw at that point. It is important to note that the wave energy device does not have braking or speed-reducing

options implemented in the design, so the voltage produced by the generator is entirely dependent on the wave conditions.

Table 2. DC Input Parameters for Custom Power Curve

	Step Number															
Parameter	**1**	**2**	**3**	**4**	**5**	**6**	**7**	**8**	**9**	**10**	**11**	**12**	**13**	**14**	**15**	**16**
Current (A)	0	20	30	40	50	51	52	53	54	55	56	57	58	59	60	61
Voltage (V)	32	33	34	35	36	40	50	60	70	80	90	100	135	170	205	240
Theoretical Power (kW)	0	0.7	1.0	1.4	1.8	2.0	2.6	3.2	3.8	4.4	5.0	5.7	7.8	10.0	12.3	14.6
Actual Power (kW)	0	0.7	1.0	1.4	1.8	1.8	1.8	1.8	1.8	1.8	1.8	1.8	1.8	1.8	1.8	1.8

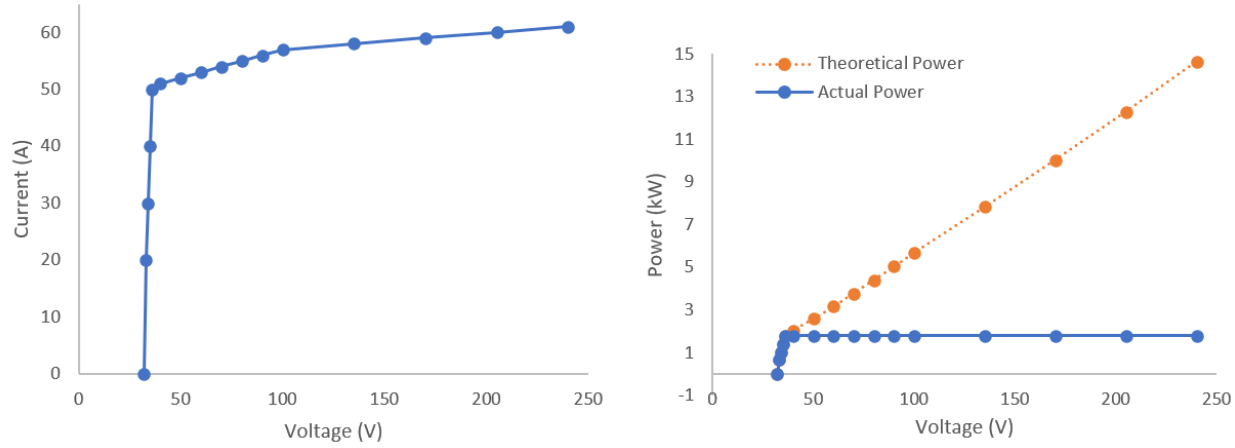

Figure 3. Custom (a) I-V curve and (b) P-V curve

2.4.3 Current Limits

The charge controller is also attached to MidNite Solar's current-sensing module, referred to as the Whizbang Junior (WBjr), which is connected to a standard 50-millivolt (mV), 500-A shunt resistor to provide amperage readings (MidNite Solar Inc. undated [a]; undated [b]). This device is used to set up a current limit on the charge controller based off the current readings from the WBjr. During programing, this device requires the desired current limit to be multiplied by 10. In the case of this system, the current limit was set to 60 A, implying that when the current into the battery exceeds 6 A, the charge controller will back its current down to maintain 6 A. Note that although the WBjr was wired into the system, it did not end up being used. Details on why are further explained in Section 2.4.4.

2.4.4 Auxiliary Ports

The charge controller includes auxiliary (AUX) ports, which can be configured to become inputs or outputs. As discussed, there is a minimum voltage required on the DC bus to maintain inverter operation; when the voltage dropped below this point, the inverter would shut off and would need to be reset manually. To ensure continuous operation, one of the auxiliary ports was used as

a power supply to a relay component, which was added between the inverter and the pump. This mechanism was put in place to allow time for the battery to recharge and keep the inverter powered, before the large pump current draw. This also protects the batteries during unenergetic sea conditions. The AUX port was programmed to operate based on the voltage of the battery, which turns the AUX output off, or disconnects from the pump, when the battery voltage would reach a low-voltage set point, and turns it on, or connects to the pump, once the battery voltage reaches a high-voltage set point. For this design, the low voltage was set to 22.6 V and the high voltage was set to 28 V. Because the inverter is primarily powered from the batteries, the relay switched off when the battery voltage dropped below 22.6 V and switched back on when the battery voltage reached 28 V.

Calibration and Troubleshooting

Much of the in-lab calibration and troubleshooting was on programming of the charge controller. Because the AUX1 port was controlling the signal to the relay that connects or disconnects the circuit from the load, the programming set points had to be calibrated carefully to the expected sea state to ensure the inverter remained powered.

Originally, the AUX1 port was programmed to operate based on the state of charge (SOC) of the battery. The "low" SOC percent set point was set to 50% and the "high" SOC percent was set to 90%, meaning the AUX1 port would output 0 V when the batteries reached 50% SOC and 12 V once the batteries charged up to 90% SOC. The charge controller would utilize the WBjr current sensor to accurately measure the current SOC of the batteries; however, after much troubleshooting, it was concluded that this configuration did not work well for the system setup and wave energy application. Because wave energy is never operating at a "steady-state" condition, the WBjr was not able to accurately determine the "steady-state" condition of the batteries.

The alternative option was to program the AUX1 to operate based on the battery voltage rather than an SOC, through what MidNite Solar refers to as "diversion" mode. This mode turns AUX1 on when it reaches the "V-HIGH" set point and turns it off once it reaches the "V-LOW" set point. After much calibration, the V-HIGH limit was set to 28 V and the V-LOW limit was set to 22.6 V. Although this option ended up being much more reliable for the application, these set points will need to be modified for different deployments depending on the sea state (MidNite Solar Inc. undated [b]). During energetic sea state conditions where the generator can consistently produce voltage above the cut-in voltage (32 V) and can charge the batteries quickly, the set points can be adjusted to gain a wider operating range and achieve longer pump run time and more water production.

3 Data Acquisition System Overview

An important part of the electrical design was the data acquisition (DAQ) system implemented to measure critical parameters. Using the Campbell Scientific CR6 data logger from Campbell Scientific (undated) and a variety of electrical sensors, the DAQ system measured the AC current and voltage produced from the generator, the DC current and voltage output from the MPPT charge controller, and the rate of water flow and pressure from the pump to the reverse osmosis unit. A detailed list of the sensors used are shown in Table 3. The design of the DAQ system and results from these measurements are made available to the public for technology benchmarking. Further detail showing where these sensors are wired throughout the system are displayed in Appendix B.

Table 3. DAQ System Channel List for Device

Channel Name	Measurement Units	Sensor Output (V)	Sensor Part Number	Description
CS1-ENC-I-P1	Amps	0–5	CR5410S-30	AC current produced from generator (phase 1)
CS2-ENC-V-P1	Volts	0–10	IsoBlock V-1C	Voltage output from generator (phase 1)
CS3-MPPT-I	Amps	0–10	DCT100-10B-24-S	DC current output from MPPT
CS4-MPPT-V	Volts	0–10	IsoBlock V-1C	DC voltage output from MPTT
CS5-FLOW	Gallons/min	0–10	SM8601	Rate of water flow from pump to reverse osmosis unit
CS6-PRESSURE	PSI	0.5–4.5	PU8503	Pressure of water from pump to reverse osmosis unit

4 Testing

The objective of the in-lab testing was to validate the operation of the hydraulic and electrical configurations. The results of this test were recorded and processed and are detailed in Section 4.4.

4.1 Test Setup

The in-lab testing required a mechanism to mimic the wave motion, which was done through a motor drive setup. As illustrated in Figure 4, the setup is powered from a 129/208-V outlet through an AC disconnect switch (rated at 40 A), to an enclosure consisting of fuses (rated at 30 A) feeding into a motor drive (Allen Bradley, Ultra3000) to drive a motor (Allen Bradley, 193481) to drive the winch drum. Between the motor and winch is a torque transducer (Eaton, 1104), which is a sensor that converts torsional mechanical input into an electrical output signal and is critical in understanding the torque production from the motor (Honeywell 2014). Connected to the motor drive is a DAQ system used for understanding voltages and currents throughout the system to help validate system operation and assist with troubleshooting during the testing phase. Figure 5 shows a visual representation of the test setup, starting from the Allen Bradley motor. Photos of the actual drive system and test set up are shown in Appendix C.

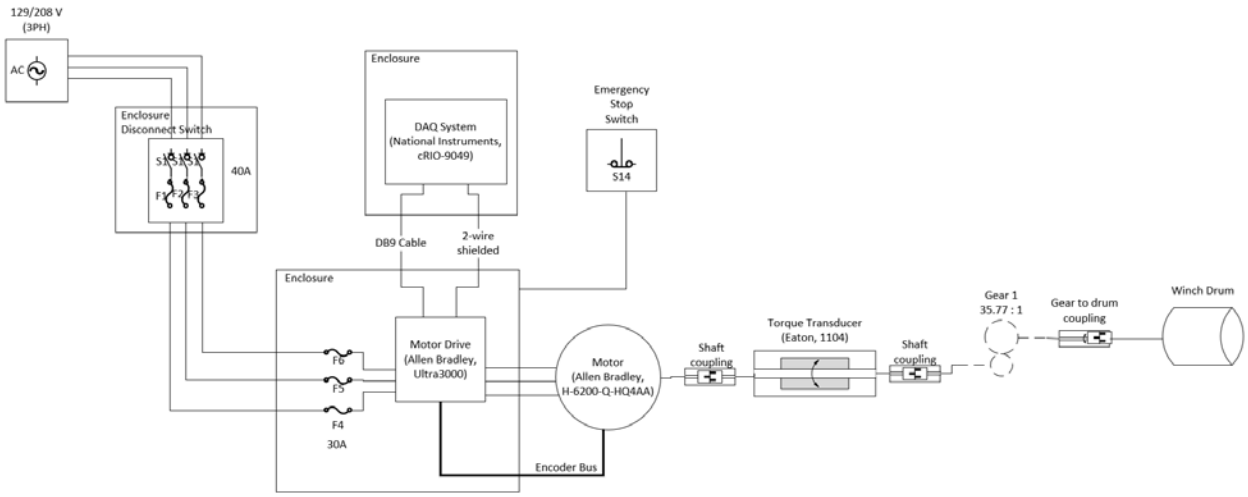

Figure 4. Wiring diagram of test setup

Figure 5. Visual display of test setup (starting from motor)

4.2 In-Lab DAQ System and Measurements

The test setup included another DAQ system using a National Instruments CompactRIO (9049) and various National Instruments measurement sensors to record measurements from ammeters, voltmeters, and a torque transducer throughout the system (National Instruments Corp undated). The setup allows for the voltages, currents, and efficiencies at each stage of the charge process to be recorded. While the motor-side drive recorded the torque delivered by the motor, a torque transducer was also added between the motor and generator to account for any error or discrepancies. Further detail showing where these sensors are wired throughout the system is displayed in Appendix D.

Table 4. DAQ System Channel List for In-Lab Testing

Channel Name	Measurement Units	Sensor Output (V)	Module Model	Channel Number	Sensor Model	Description
gD1-En	N·m	0–10	NI 9237	CH-0	1104	Torque from motor to gearbox
gD8-ENC-I-P1	Amps	0–5	NI 9239 (2)	CH-2	CR5410S-30	AC current after subsea cable (phase 1)
gD9-ENC-I-P2	Amps	0–5	NI 9239 (2)	CH-3	CR5410S-30	AC current after subsea cable (phase 2)
gD10-ENC-I-P3	Amps	0–5	NI 9239 (3)	CH-0	CR5410S-30	AC current after subsea cable (phase 3)
gD11-ENC-V-P1	Volts	0–10	NI 9239 (3)	CH-1	IsoBlock V-4C	AC voltage after subsea cable (phase 1)
gD12-ENC-V-P2	Volts	0–10	NI 9239 (3)	CH-2	IsoBlock V-4C	AC voltage after subsea cable (phase 2)
gD13-ENC-V-P3	Volts	0–10	NI 9239 (3)	CH-3	IsoBlock V-4C	AC voltage after subsea cable (phase 3)
gD14-MPPT-V	Volts	0–10	NI 9239 (4)	CH-0	IsoBlock V-1C	DC voltage output from MPPT
gD15-MPPT-I	Amps	0–10	NI 9239 (4)	CH-1	DCT100-10B-24-S	DC current output from MPPT
gD16-BATT-I	Amps	0–10	NI 9239 (4)	CH-2	DCT100-10B-24-S	DC current draw from batteries
gD17-BATT-V	Volts	0–10	NI 9239 (4)	CH-3	IsoBlock V-1C	DC voltage input to batteries
gD18-INV-V	Volts	0–10	NI 9239 (5)	CH-0	IsoBlock V-1C	DC voltage input to inverter
gD19-PUMP-V	Volts	0–10	NI 9239 (5)	CH-1	IsoBlock V-1C	AC voltage input to pump
gD20-PUMP-I	Amps	0–5	NI 9239 (5)	CH-2	CR4110-25	AC current draw from pump

4.3 Testing Conditions

To mimic a variety of possible sea state conditions, various sinusoidal waveforms were developed in MATLAB to drive the Allen Bradley motor in the test setup. Table 5 lists the details of the various waveforms tested in-lab, where the gear ratio between the motor drive and winch is 35.77:1 and the gear ratio between the winch and generator is 1:11.28 (refer to Appendix D). As detailed in Table 5, the first waveform that was tested was a large-period (20 seconds [s]), small-amplitude (0.5 meter [m]) sine wave, which resulted in a slow max rotational speed of 95 rpm at the generator to ensure the system operated as expected when power was supplied and a basic sine wave was inputted. Once validated, testing conditions got progressively faster, and various wave periods and heights were tested for each condition. The highest motor drive speed tested was a 7-s wave period with a maximum motor drive speed of 2,200 rpm, resulting in a speed at the generator of 694 rpm. The maximum wave period was limited by both the maximum motor drive speed and the length of the cable on the drive system, which was approximately 5 m long. Because distance is the product of speed and time, a maximum wave

height (H) of 1.43 m, which represents heave travel, and wave period (T) of 7 s were tested to maintain a safe limit with the cable.

Table 5. List of Various Tested Waveforms for In-Lab Testing

Test #	T (s)	H (m)	Max Drive Speed (rpm)	Winch Speed (rpm)	Generator Speed (rpm)
1	20	0.5	300	8	95
2	40	1.49	400	11	126
3	10	0.5	600	17	189
4	20	1.1	600	17	189
5	16	1.19	800	22	252
6	12	1.1	1,000	28	315
7	5	0.5	1,200	34	378
8	10	1.1	1,200	34	378
9	18	2	1,200	34	378
10	8	1.1	1,400	39	441
11	6	0.95	1,700	48	536
12	5	0.9	2,000	56	631
13	7	1.3	2,000	56	631
14	7	1.43	2,200	62	694

4.4 Experiments and Results

This section reports on the experimental results and performance assessment of the WEC's electrical PTO. The data from each sensor throughout the electrical system were recorded, processed, and graphed. Figure 6 displays the measurements for the largest waveform (line 14 from Table 5), which was run at 2,200 rpm at the drive motor, with a significant wave height, H = 1.43 m, and with a wave period of T = 7 s. This test was selected because it clearly illustrates the control strategy of the charge controller and overall system. The following sections (4.4.1–4.4.4) will step through various segments of the data to explain how the control strategy was designed to function.

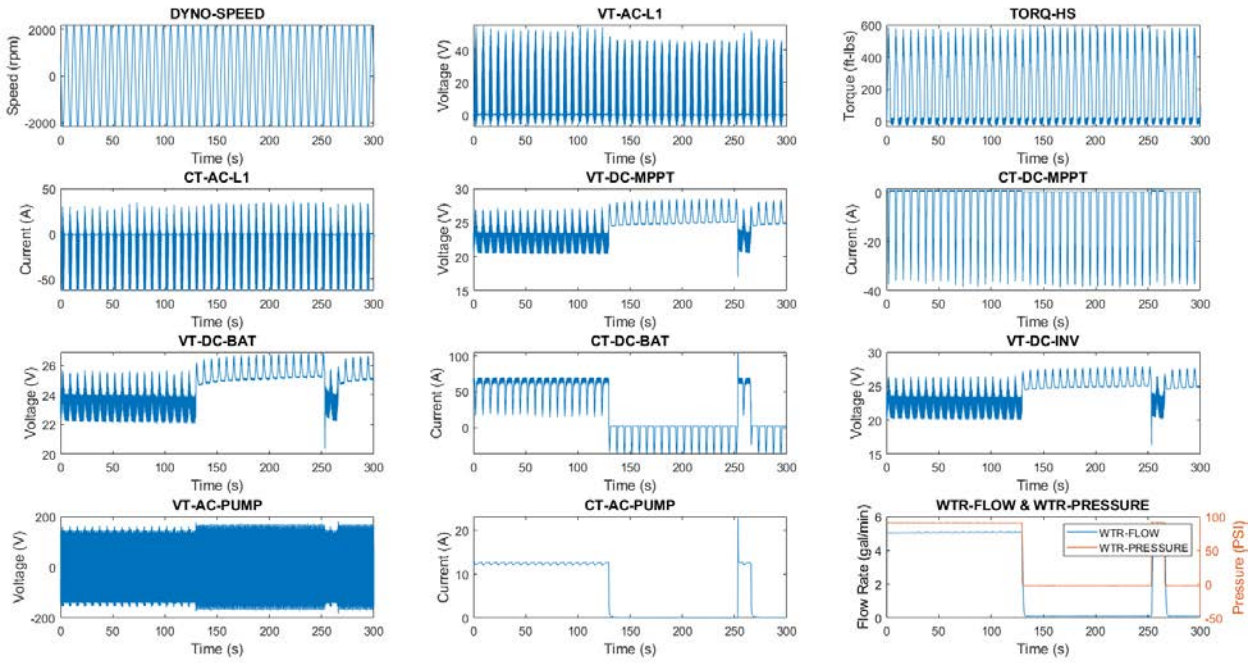

Figure 6. Summary of measurements from in-lab testing

4.4.1 Voltage and Current Relationships

In an electric generator, voltage produced is directly proportional to its rotational speed (in revolutions per minute). Figure 7 zooms in on the dynamometer (dyno) speed and voltage produced by the generator (phase 1) to illustrate the relationship between the two. As shown in the figure, the generator is only producing voltage when the dyno speed waveform is in the negative direction and is zero when the dyno speed approaches the positive region. This is because a one-way clutch mechanism was inputted into the design of this WEC, which only allows for generator shaft rotation, and therefore voltage production, in one direction. A clutch was used to enable the WEC to extract energy in the heave direction, while allowing the spring mechanism to rewind the winch on the down stroke, repeating the cycle. Similarly, in an electrical generator, torque and current draw are proportional to one another—Figure 8 illustrates the relationship between the two. It is important to note that the AC voltage (VT-AC-L1) and current (CT-AC-L1) waveforms are not symmetrical around zero. The reason for this has not been proven at this time but will be addressed with further testing as NREL plans to continue to improve the system design and better understand the research area gaps that exist.

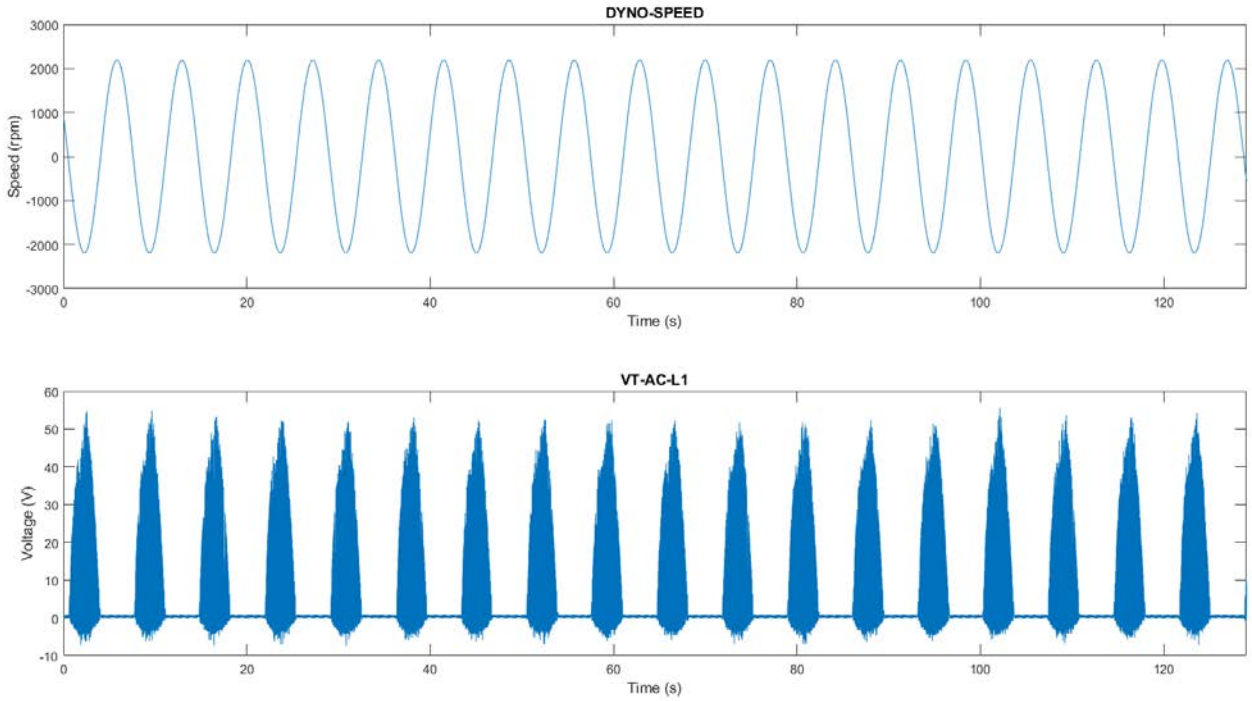

Figure 7. Dyno speed vs. generator voltage

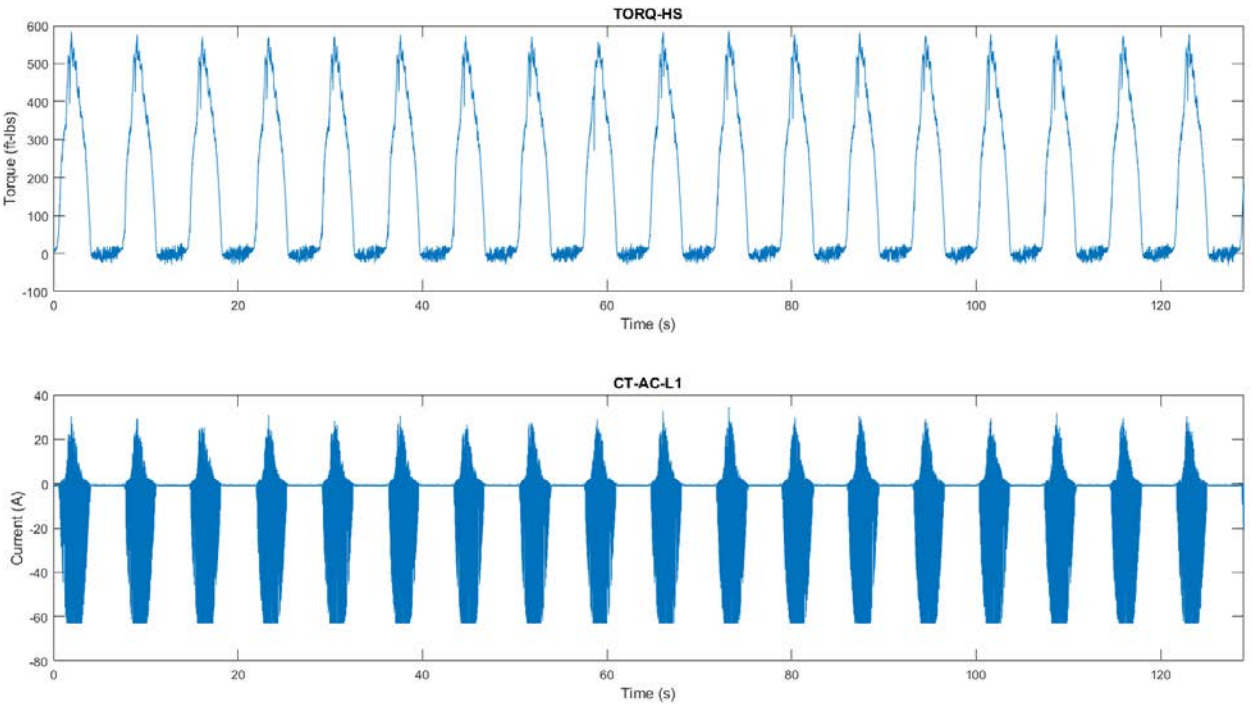

Figure 8. Torque vs. current draw

4.4.2 Steady State: Pump Is ON

Figure 9 shows the voltage waveforms zoomed in from 0 to 20 s, which is the segment of the test run where the pump is on and water is flowing (refer to the fifth and sixth plots from the top of the figure). As clearly depicted in the first and third plots, when there is not a voltage generation pulse from the generator, the battery voltage dips due to the high draw of current from the load, or the pump. Conversely, when there is power generated by the WEC during actuation, and subsequently power from the MPPT, the voltage at the battery increases (refer to the third plot) as determined by the MPPT voltage set point. The voltage profiles of the MPPT charge controller (second plot) and inverter (fourth plot) experience a similar trend, as they are all connected to the same 24-V DC bus.

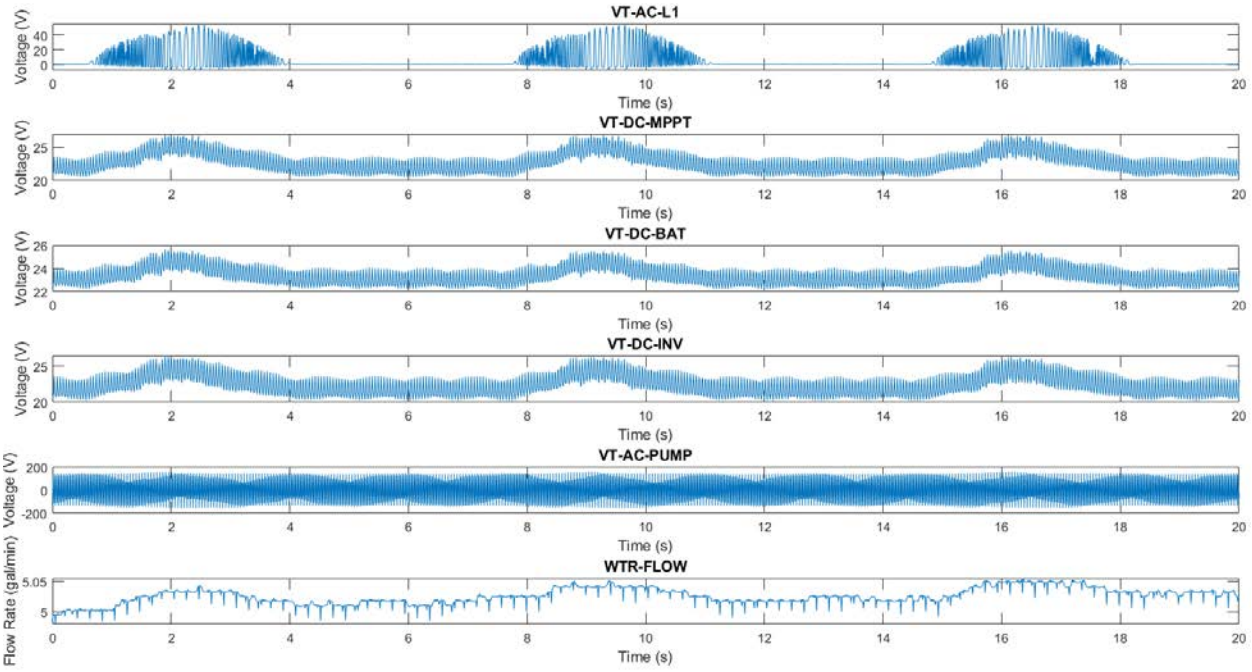

Figure 9. Steady-state condition when pump is on

4.4.3 Transient State: Pump Turns OFF

Figure 10 shows the voltage waveforms zoomed in from 120 to 140 s, which is the segment of the test run where the battery voltage drops below the critical voltage set point and the control strategy of the charge controller kicks in. At 129 s, the battery voltage drops below 22.6 V, the AUX port turns off and the relay disconnects the inverter from the pump, causing the pump to turn off, or the water to stop flowing, to allow the batteries to charge enough until it reaches the high critical voltage set point of 28 V. As mentioned in Section 2.4.4, this mechanism was put in place to allow time for the battery to recharge and be capable of keeping the inverter powered, before the large pump current draw. Note that there is a 1–2 second delay between the voltages seen by the MPPT and when the AUX control kicks in.

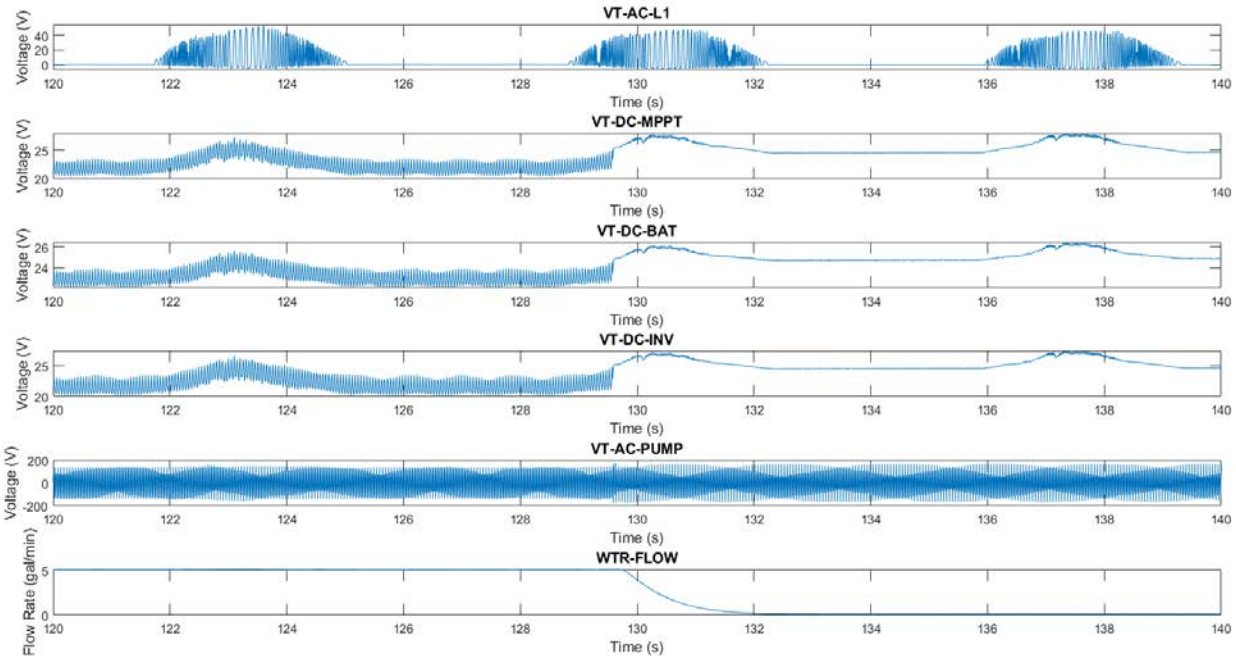

Figure 10. Transient state condition when pump turns off

4.4.4 Transient State: Pump Turns On

Figure 11 shows the voltage waveforms zoomed in between 250 to 270 s, which is the segment of the test run where the pump temporarily turns back on when the battery voltage reaches its maximum critical point, as expected. However, once the battery voltage drops below the minimum critical point, the control mechanism kicks in, the pump turns back off, and the same pattern is repeated.

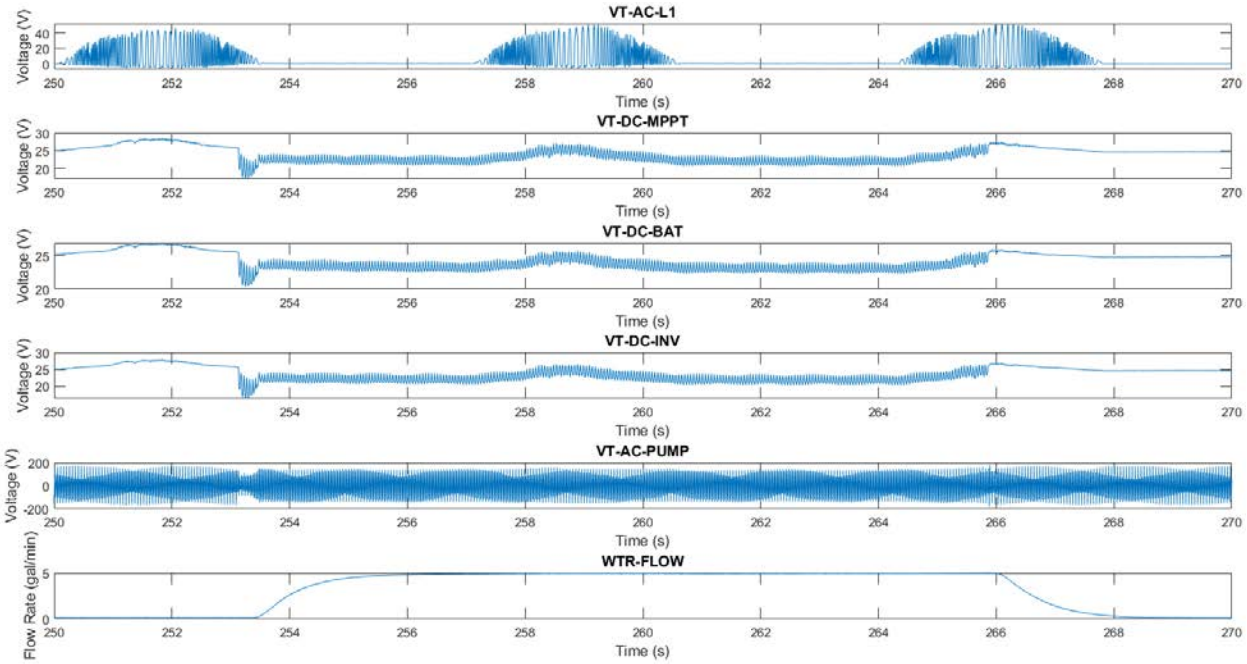

Figure 11. Transient state condition when pump turns on

5 Cost Summary

The costs of the individual components that went into building the electrical piece of the wave device and the DAQ system are documented. Table 6 shows the total cost and summary of the categorical costs; each component is labeled as its corresponding category type. A detailed list of individual components, part numbers, suppliers, and unit costs can be found in Appendix E. Figure 12 provides a visual breakdown of the categorical costs. Note that some of these costs may include shipping costs.

Table 6. Summary of Categorical Costs

Category	Cost	Percentage
Generator	$3,800.00	12%
Subsea Cable	$4,475.00	14%
Pump	$700.31	2%
Electrical Conversion/Controllers	$4,806.84	15%
Battery Storage (WEC)	$540.00	2%
Power Supply (DAQ)	$540.00	2%
Sensors/DAQ	$3,660.38	11%
Circuit Protection/Switches	$6,805.93	21%
Wiring/Connection	$3,877.60	12%
Structural Assembly	$3,000.00	9%
Total Cost	**$32,206.06**	**100%**

As indicated in Figure 12, the highest cost category (21%) is circuit protection/switches, which includes the electrical enclosures, disconnect switches, fuses/ground fault circuit interrupter, circuit breakers, and the relay. The second highest cost category (15%) is the electrical conversion/controller components, which include the charge controller, inverter, rectifier, DC-DC converter, and voltage-reducing device. The subsea cable, separate from the wiring/connection category, is the next highest cost (14%) in the system. The following three categories all have roughly the same total cost (11%–12%): wiring/connection (wiring inside the enclosure and necessary connectors, like ferrules, terminals, etc.); the generator; and sensors/DAQ (sensors and data logger for the DAQ on the WEC). The remaining cost categories include the structural assembly, estimated at about 9% of the overall cost; the pump, which also includes the pump's control and protector; battery storage for the WEC; and the power supply for the DAQ system, which consists of another, larger battery bank.

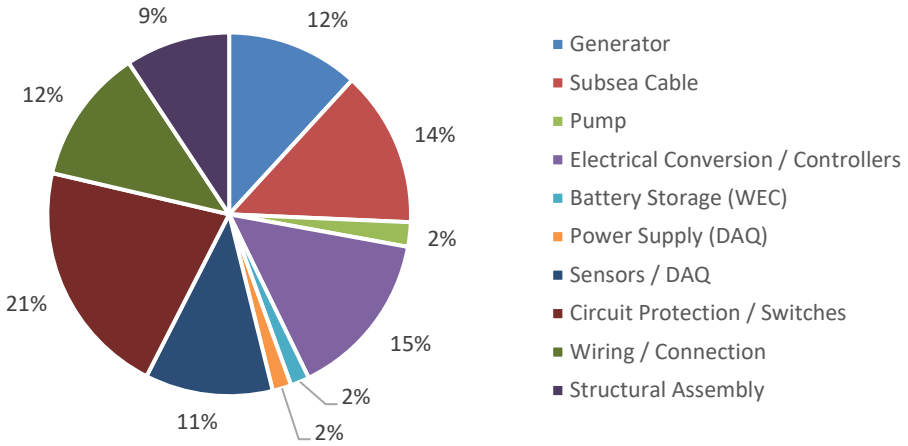

Figure 12. Breakdown of categorical costs

To provide a uniform platform to estimate the capital and operational costs that accrue for marine energy technology projects, the WPTO developed a system cost breakdown structure (CBS) template, which is linked at OpenEI[1] (2022). This framework is used as a standardized cost reporting framework to facilitate uniform categorization of subsystems and components. This framework serves as the basis for many levelized cost of energy calculations. It covers all life cycle expenditure categories, including the costs associated with project planning, permitting, generating equipment, supporting infrastructure, and operations and maintenance, among many others. The hierarchy in the CBS consists of six levels, starting from more general to increasingly specific categories. The detailed levels of the CBS (Levels 4 and 5) contain cost elements that are only applicable to some technologies. Figure 13 shows how the cost categories in Table 6 for the HERO WEC system can be mapped to Level 4 categories in WPTO's CBS.

WEC Category
Generator
Subsea Cable
Pump
Electrical Conversion / Controllers
Battery Storage (WEC)
Power Supply (DAQ)
Sensors / DAQ
Circuit Protection / Switches
Wiring / Connection
Structural Assembly

CBS Category	CBS #
Generator	1.1.2.4
Power Electronics	1.1.2.6
Additional Structural Components	1.1.1.2

Figure 13. Cost categories mapped to WPTO CBS

[1] https://openei.org/wiki/PRIMRE/Guidelines#LCOE

6 Future Work

There was much uncertainty in how a commercial off-the-shelf charge controller would function in a wave energy application with highly irregular conditions. To the team's knowledge this was the first time such a controller was used in a wave energy application. To gain further understanding of how different charge controller types (pulse-width modulation and MPPT) operate with irregularity in wave direction, amplitude, and frequency, NREL will perform a validation exercise comparing their performances and efficiencies. The results from this project will be published and made available to the public for technology benchmarking and to provide a reference point for future developers. NREL will continue to test the system to validate its performance and publish results.

While commercial off-the-shelf components can be used in a functioning WEC, there is a substantial need for bespoke power electronics and power conversion systems that can manage the wide range of operating conditions common to wave energy. It is strongly recommended that focused research and development is performed to support the proliferation and adoption of wave energy technologies into the renewable energy portfolio at both Powering the Blue Economy™ and grid scale. Specifically, robust power electronics must be developed that are capable of sustained operation at very low power points, have high efficiency over a wide operating range, and are capable of continued operation through extreme, or peak, events.

References

Campbell Scientific. undated. "CR6 Measurement and Control Datalogger." https://www.campbellsci.com/cr6.

Honeywell. 2014. "Model 1104 to 1107 Standard Rotating Shaft Torque Sensor." https://prod-edam.honeywell.com/content/dam/honeywell-edam/sps/siot/ru-ru/products/test-and-measurement-products/torque-transducers/slip-ring/model-1100-series/documents/sps-siot-t-m-model-1104-1107-rotate-shaft-torque-datasheet-008771-2-en-ciid-152077.pdf.

MidNite Solar Inc. undated (a). "MNWBJR WhizBang Jr." https://www.midnitesolar.com/productPhoto.php?product_ID=519&productCatName=Other&productCat_ID=43&sortOrder=1&act=p.

MidNite Solar Inc. undated (b). "CLASSIC 250." https://www.midnitesolar.com/productPhoto.php?product_ID=258&productCatName=Wind%20and%20Hydro&productCat_ID=25&sortOrder=1&act=p.

National Instruments Corp. undated. "cRIO-9049 CompactRIO Controller." https://www.ni.com/en-us/support/model.crio-9049.html.

OpenEI. 2022. "Levelized Cost of Energy (LCOE) Guidance." https://openei.org/wiki/PRIMRE/Telesto/LCOE.

Phocos. 2015. "Comparing PWM & MPPT Charge Controllers." https://www.phocos.com/wp-content/uploads/2019/11/Guide-Comparing-PWM-MPPT-Charge-Controllers.pdf.

Appendix A. Custom Generator Assembly Drawing

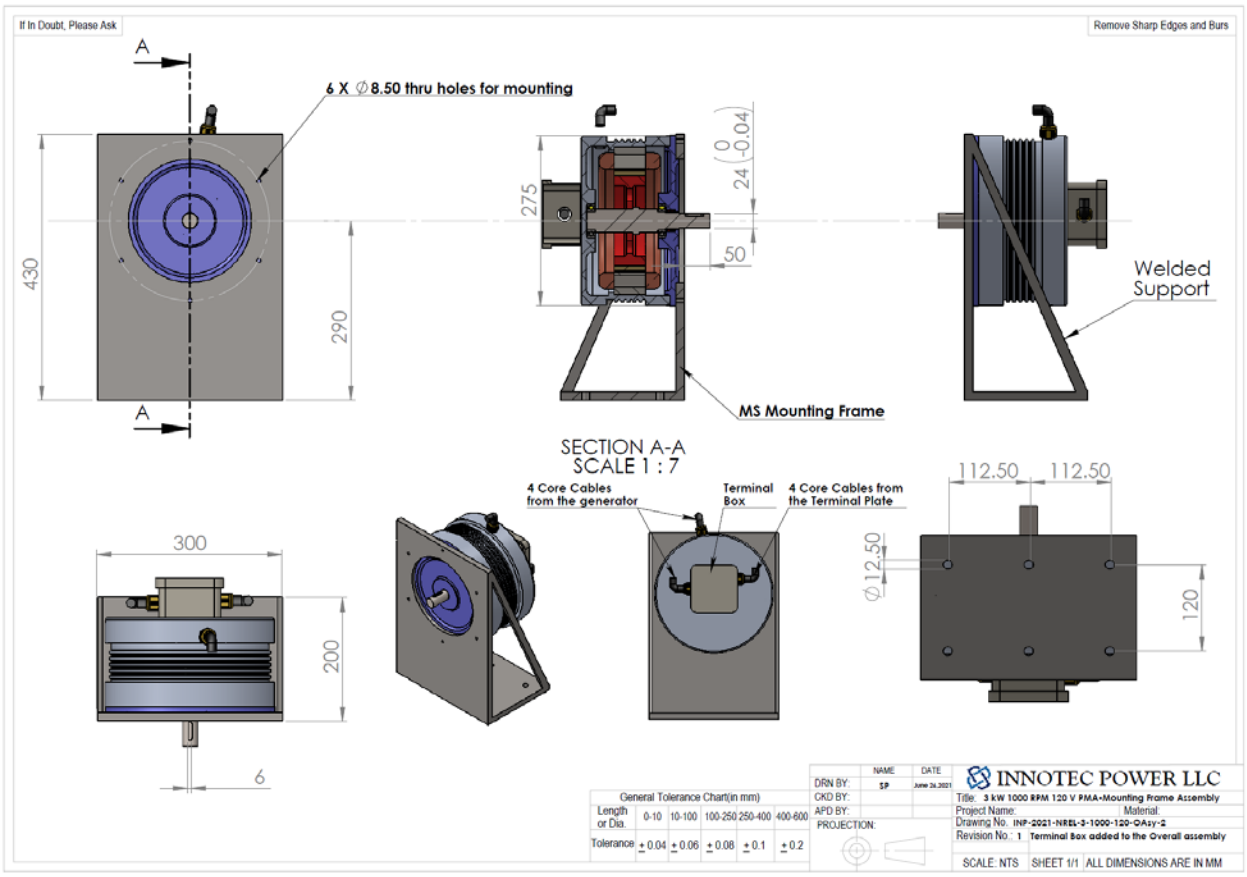

Figure A-1. Custom generator assembly drawing

Appendix B. Full Wiring Diagram for Deployment

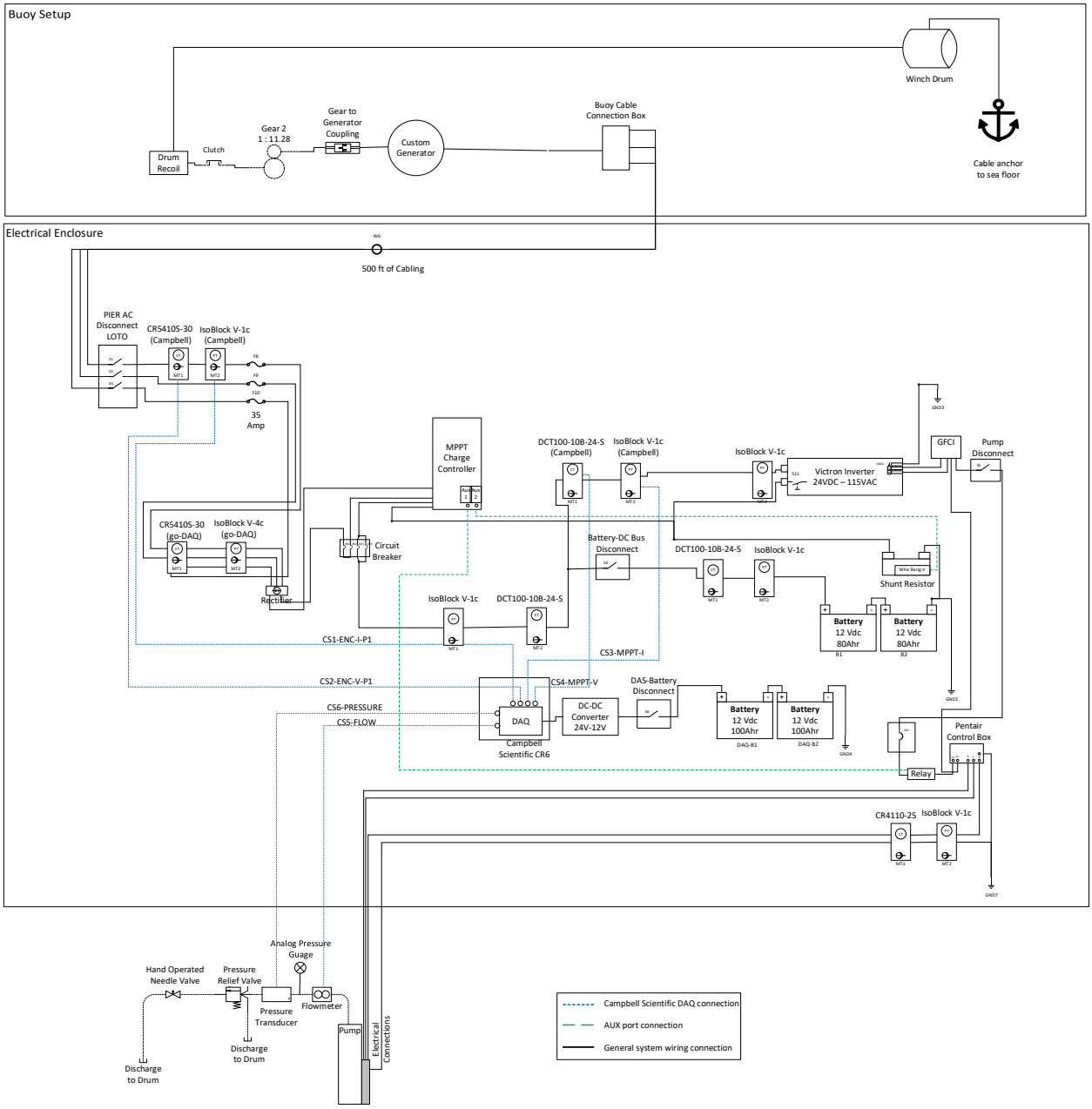

Figure B-1. Electrical wiring diagram

Appendix C. In-Lab Test Setup

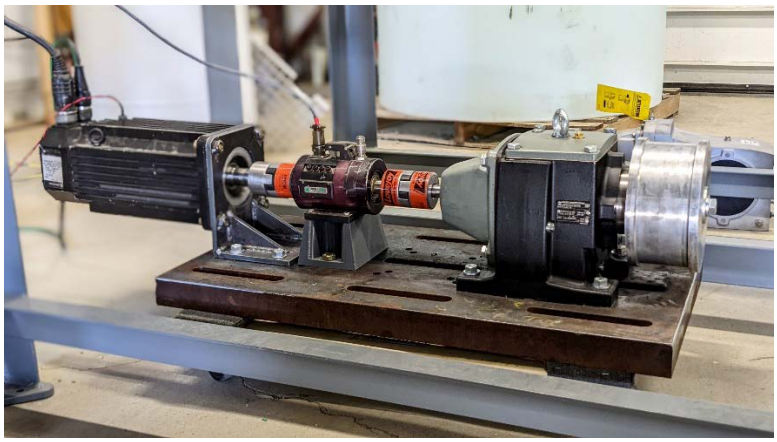

Figure C-1. Drive system setup

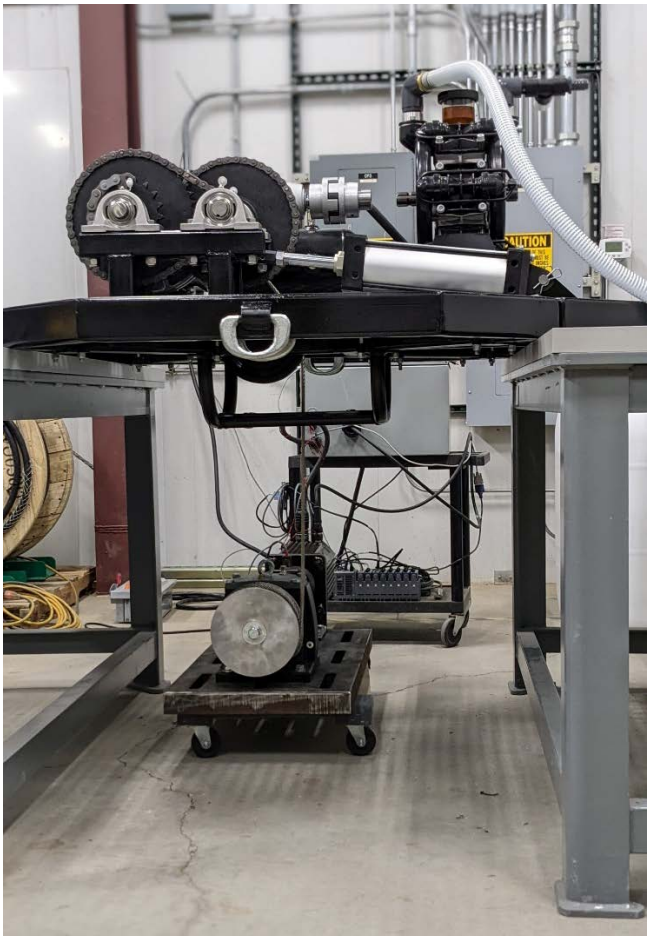

Figure C-2. WEC and drive system setup

Appendix D. Full Wiring Diagram for In-Lab Testing

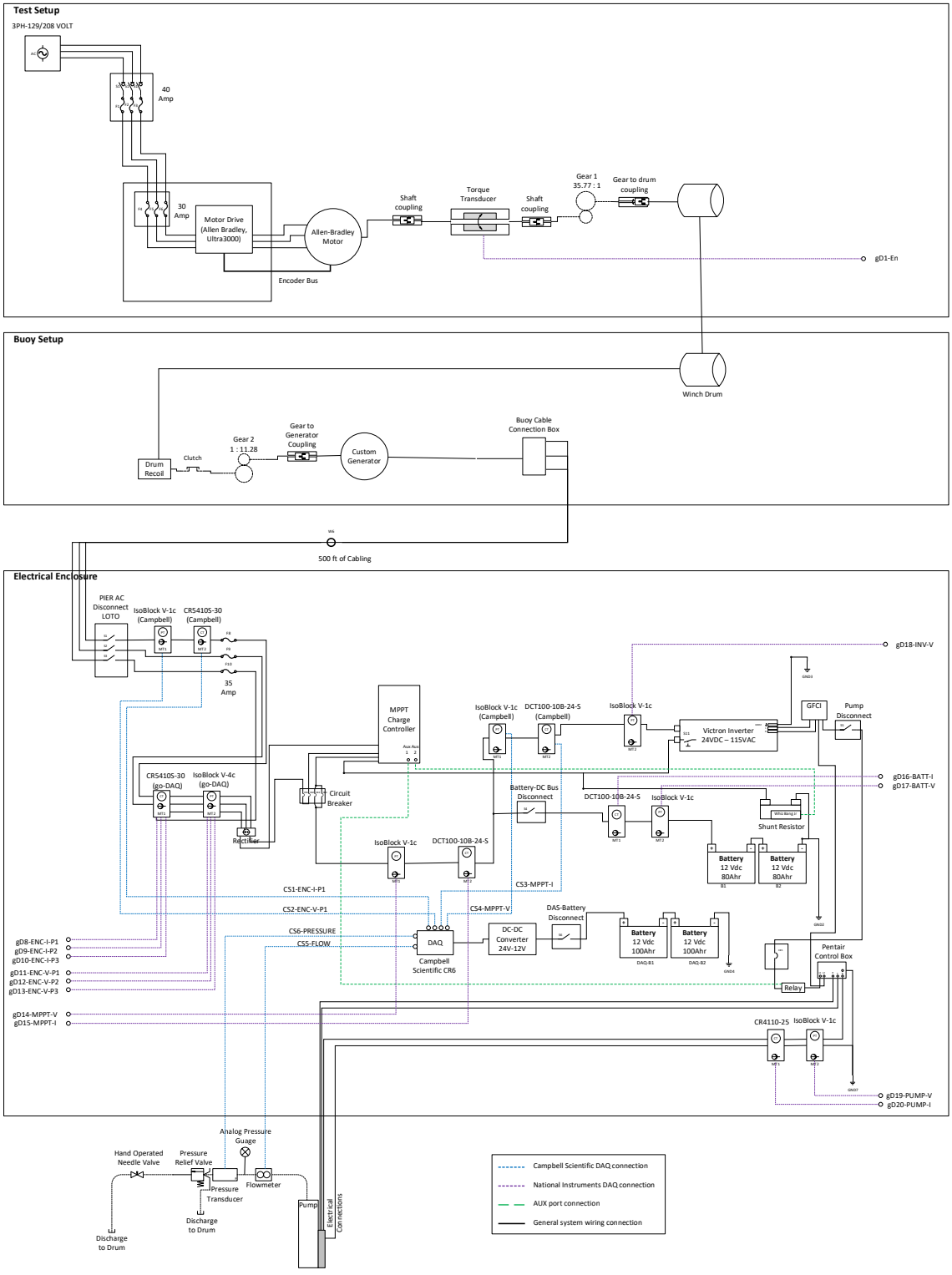

Figure D-1. Test setup with measurements and channel names

Appendix E. Single Unit Cost Breakdown of Components

#	Component	Category	Brand	Part Number	Company / Supplier	Cost/Unit	Quantity	Total Cost
1	Electrical PTO Enclosure	Circuit Protection / Switches	DBB Unlimited	OD-30DDC	DDB Unlimited	$ 2,933.33	1	$ 2,933.33
2	Generator / junction box	Generator	Innotec Power	custom	Innotec Power	$ 2,900.00	1	$ 3,800.00
3	Generator connector	Wiring / Connection	Innotec Power	131-LP-24-C04SX-03-401	Innotec Power	$ 380.00	1	$ 380.00
4	Subsea cable	Subsea Cable	Draka	NNC13512X	Anixter	$ 4,475.00	1	$ 4,475.00
5	AC Disconnect (LOTO)	Circuit Protection / Switches	Katko	KEM380UL	Allied Electronics	$ 205.00	1	$ 205.00
6	AC/DC current transducer	Sensors / DAQ	CR Magnetics Inc.	CR5410S-30	DigiKey	$ 221.55	2	$ 443.10
7	Voltage sensor (1400V max)	Sensors / DAQ	Verivolt	IsoBlock V-1c	Verivolt	$ 260.00	2	$ 520.00
8	Fuses (35 A)	Circuit Protection / Switches	-	-	-	$ 1,500.00	-	$ 1,500.00
9	Charge controller	Electrical Conversion / Controllers	MidNite Solar	CLASSIC250	Missouri Wind and Solar	$ 785.40	1	$ 785.40
10	DC Disconnect (battery)	Circuit Protection / Switches	Aims Power	DC1600V32A2IO	Amazon	$ 114.00	1	$ 114.00
11	Shunt resistor	Sensors / DAQ	MidNite Solar	SHUNT-500A-50MV	Missouri Wind and Solar	$ 37.08	1	$ 37.08
12	Whiz bang jr	Sensors / DAQ	MidNite Solar	MNWBJR	Missouri Wind and Solar	$ 60.20	1	$ 60.20
13	Inverter	Electrical Conversion / Controllers	Victron	PIN243020100	Inverters R Us	$ 1,569.95	1	$ 1,569.95
14	GFCI	Circuit Protection / Switches	Hubbell	HUBGFHW13115	Amazon	$ 407.00	1	$ 407.00
15	AC Disconnect (pump)	Circuit Protection / Switches	Schneider Electric	MD3304X	Amazon	$ 145.00	1	$ 145.00
16	CR6 Data logger *	Sensors / DAQ	Campell Scientific	CR6	Fisher Scientific	$ 2,600.00	1	$ 2,600.00
17	DC-DC Converter	Electrical Conversion / Controllers	TDK-Lambda Americas Inc	DPX40-24WS12	DigiKey	$ 166.50	1	$ 166.50
18	DC Disconnect (DAS-battery)	Circuit Protection / Switches	IMO	SI16-PEL64R-2	Amazon	$ 75.00	1	$ 75.00
19	Rectifier	Electrical Conversion / Controllers	Crydom	M5060TB1600	Master Electronics	$ 85.00	1	$ 85.00
20	Battery (DAQ) - 100Ah	Power Supply (DAQ)	Renogy	RNG-BATT-AGM12-100-US	Renogy	$ 270.00	2	$ 540.00
21	Battery (WEC) - 88 Ah	Battery Storage (WEC)	Optima	DH7	Auto Zone	$ 270.00	2	$ 540.00
22	Circuit breakers	Circuit Protection / Switches	-	-	-	$ 300.00	-	$ 300.00
23	Relay	Circuit Protection / Switches	TE Connectivity Potter & Brumfield Relays	KUHP-5D51-12	DigiKey	$ 23.92	1	$ 23.92
24	Control box	Wiring / Connection	Pentair	PTKSMCIR0511	RC Worst Co	$ 111.30	1	$ 111.30
25	Charge Controller Kit	Electrical Conversion / Controllers	Missouri Wind and Solar	CBSUCLASSICVRD	Missouri Wind and Solar	$ 2,199.99	1	$ 2,199.99
26	Pin & sleeve female connector	Wiring / Connection	Scame	SCM460C7W	ElecDirect	$ 174.03	1	$ 174.03
27	Pin & sleeve male inlet	Wiring / Connection	Scame	SCM460B7W	ElecDirect	$ 135.19	1	$ 135.19
28	Receptacle box	Wiring / Connection	Scame	SCMBB02	ElecDirect	$ 77.08	1	$ 77.08
29	Enclosure for umbilical cable	Circuit Protection / Switches	-	-	-	$ 1,102.68	1	$ 1,102.68
30	Wiring	Wiring / Connection	-	-	-	$ 1,000.00	1	$ 1,000.00
31	Connectors	Wiring / Connection	-	-	-	$ 2,000.00	1	$ 2,000.00
32	Structural assembly	Structural Assembly	Various	-	-	$ 3,000.00	1	$ 3,000.00
33	Pump	Pump	Berkeley	B5P4MS05131-01	PumpProducts.com	$ 455.50	1	$ 455.50
34	Pump control	Pump	Berkeley	SMC-IR0511-03	PumpProducts.com	$ 67.89	1	$ 67.89
35	Pump protector	Pump	Berkeley	SPP-11P-3RL	PumpProducts.com	$ 176.92	1	$ 176.92
							Total Cost	$ 32,206.06

Figure E-1. Bill of materials